npg

Non-small cell lung cancer stem/progenitor cells are enriched in multiple distinct phenotypic subpopulations and exhibit plasticity

S Akunuru[1,2], Q James Zhai[3] and Y Zheng*[,1,2]

Cancer stem cells (CSCs) represent a population of cancer cells that possess unique self-renewal and differentiation characteristics required for tumorigenesis and are resistant to chemotherapy-induced apoptosis. Lung CSCs can be enriched by several markers including drug-resistant side population (SP), CD133^{pos} and ALDH^{high}. Using human non-small cell lung adenocarcinoma cell lines and patient-derived primary tumor cells, we demonstrate that SP cells represent a subpopulation distinct from other cancer stem/progenitor cell (CS/PC) populations marked by CD133^{pos} or ALDH^{high}. The non-CS/PCs and CS/PCs of each subpopulation are interconvertible. Epithelial-mesenchymal transition (EMT) promotes the formation of CD133^{pos} and ALDH^{high} CS/PC subpopulations while suppressing the SP CS/PC subpopulation. Rac1 GTPase activity is significantly increased in cells that have undergone EMT, and targeting Rac1 is effective in inhibiting the dynamic conversion of non-CS/PCs to CS/PCs, as well as the CS/PC activity. These results imply that various subpopulations of CS/PCs and non-CS/PCs may achieve a stochastic equilibrium in a defined microenvironment, and eliminating multiple subpopulations of CS/PCs and effectively blocking non-CS/PC to CS/PC transition, by an approach such as targeting Rac1, can be a more effective therapy.
Cell Death and Disease (2012) **3,** e352; doi:10.1038/cddis.2012.93; published online 19 July 2012
Subject Category: Cancer

The cancer stem cell (CSC) theory predicts that a fraction of cancer cells possess unique self-renewal properties that mediate tumor initiation and propagation.[1] Consistent with this theory, several cell subpopulations have been identified by either cell surface markers or enzymatic activities as CSCs in solid tumors. Previous studies demonstrated the CSC's drug resistance,[2–4] self-renewal characteristics and tumor-initiating properties in xenograft mouse models.[5–9] In lung cancer, three different marker-defined CSC populations have been identified: drug-resistant side population (SP),[3,10] CD133^{pos} cells[2,11] and ALDH^{high} cells.[12,13] SP cells isolated from non-small cell lung adenocarcinoma (NSCLA) cell lines had higher expression of ABC transporters and were resistant to chemotherapeutic drugs.[3] We previously showed that NSCLA SP cells were more metastatic in xenograft models and the invasive behavior of SP cells was driven by high Rac1 activity.[10] Drug-resistant cells derived from NSCLA cell lines were enriched for CD133^{pos} cells and displayed elevated cytokine expression.[11] NSCLA cells with higher ALDH activity were more tumorigenic, with elevated notch1 signaling driving the tumor-initiating activity.[13] However, the relationship between these different marker-defined cancer stem/progenitor cell (CS/PCs), that is, whether they represent overlapping, stochastic or hierarchical subpopulations of NSCLA, has not been established.

Advancement of CSC theory has led to the proposal that targeting CSCs may eradicate residual chemoradiation therapy-resistant tumor cells in patients. Consequently, Gupta *et al.*[14] suggested that induced CSC differentiation by salinomycin can block mammary CSC activity and metastasis, although the efficacy of such reagents remained untested in preclinical and clinical solid tumor models. Several recent reports propose that CSCs and non-CSCs can exhibit plasticity and interconvert in nature.[15,16] Epithelial-mesenchymal transition (EMT) was proposed as one of the underlying mechanisms for CSC generation in breast cancer.[17] Whether such properties observed in breast cancer translate to lung cancer remains unclear.

Identifying mechanisms involved in lung CSC regulation may help develop novel, effective cancer therapies. Using NSCLA cell lines and primary patient samples, we demonstrate that the SP, CD133^{pos} and ALDH^{high} cells are phenotypically distinct subpopulations enriched for CS/PC activity. Non-SP, CD133^{neg} or ALDH^{low} cells can generate SP, CD133^{pos} and ALDH^{high} cells, respectively. EMT induced by TGFβ1 or Snail elevates CD133^{pos} and ALDH^{high} subpopulations while reducing the SP subpopulation. Rac1, a Rho GTPase family member with known roles in metastasis and EMT, is activated during EMT, and Rac1 inhibition blocks EMT and the dynamic plasticity between CS/PCs and

[1]Division of Experimental Hematology and Cancer Biology, Children's Hospital Research Foundation, Children's Hospital Medical Center, University of Cincinnati, Cincinnati, OH, USA; [2]Molecular Developmental Biology Program, Children's Hospital Research Foundation, University of Cincinnati, Cincinnati, OH, USA and [3]Department of Pathology and Laboratory Medicine, University of Cincinnati, Cincinnati, OH, USA
*Corresponding author: Y Zheng, Division of Experimental Hematology and Cancer Biology, Children's Hospital Research Foundation, Children's Hospital Medical Center, University of Cincinnati, 3333 Burnet Avenue, Cincinnati, OH 45229, USA. Tel: 513 636 0595; Fax: 513 636 3768; E-mail: yi.zheng@cchmc.org

non-CS/PCs, underscoring its potential as a useful therapeutic target.

Results

NSCLA cells contain multiple, phenotypically distinct CS/PC subpopulations. To dissect the relative expression of different CS/PC markers in NSCLA cell lines, we first identified SP, CD133^{pos} and ALDH^{high} populations in A549 and H441 cells. A549 cells expressed 4–10% SP, 0.3–1% CD133^{pos} and 2–8% ALDH^{high} cells, whereas H441 cells contained 0.5–3% SP, 0.1–0.5% CD133^{pos} and 0.5–2% ALDH^{high} cells (Figure 1a). A549 cells also expressed 10–15% CD24^{low}CD44^{high}, markers associated with CSC activity in breast cancer (Supplementary Figure S1A), whereas H441 cells expressed 18–30% CD24^{low} with undetectable CD44. Further, we isolated cells from primary NSCLA tumor samples and cultured them in non-adherent sphere-forming conditions. These cells have a cobble-stone epithelial morphology in adherent culture. After 1 week in sphere-forming conditions, primary NSCLACs contain 80%

CD133^{pos} and 2% SP cells (Figure 1b, left panel). Interestingly, when cells were cultured in adherent culture conditions for an additional 1 or 3 weeks, the CD133^{pos} subpopulation decreased to either 20% or 2%, respectively, whereas the SP subpopulation increased to 8–10% and 15–18%, respectively (Figure 1b middle and right panels, respectively), suggesting the various marker-defined subpopulations of CS/PC transition dynamically.

We sought to determine the potential overlap of these different marker-defined CS/PCs in NSCLA cells. We performed FACS analysis on SP and non-SP cells to determine the expression of CD133 or ALDH. We observed minimal overlap between SP and CD133^{pos} (Figure 1c) and between SP and ALDH^{high} (Figure 1d) in both A549 cells (Figure 1c left panel, 1D left panel) and primary NSCLA cells (Figure 1c right panel, 1D right panel). The CD24^{low}CD44^{high} subpopulation was similarly distributed in SP and non-SP primary NSCLA cells (Supplementary Figure S1B). Apparently, enriching for CS/PCs with one marker set does not correlate with an enrichment of CS/PCs identified by another marker set. When the lung colonization activities of 50 000 SP cells and 10 000
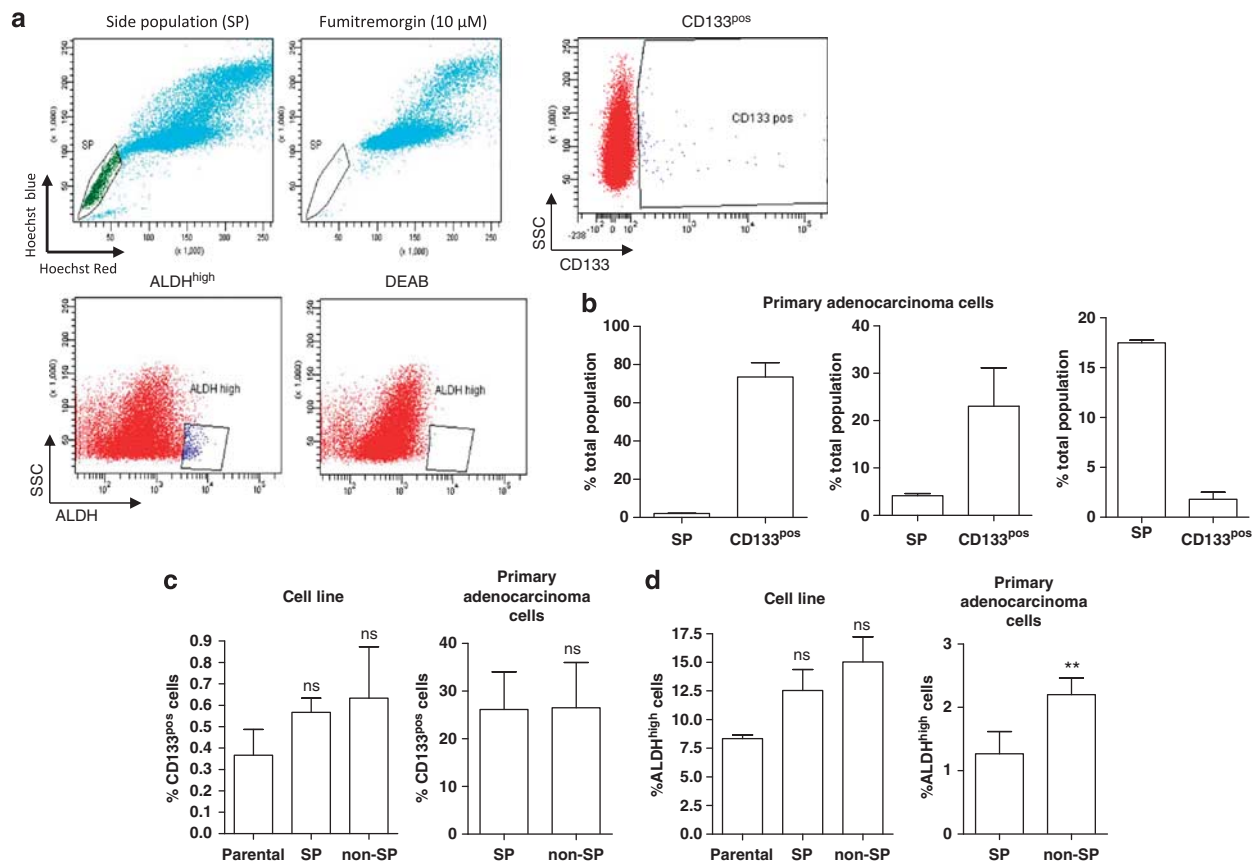

Figure 1 NSCLA cells express multiple, distinct CSC subpopulations based on markers. (**a**) A549 cells were stained with Hoechst dye for SP manifestation. Cells were stained in the presence of 10 μM Fumitremorgin as a negative control (left panel). A549 cells were stained with CD133 antibody and analyzed by FACS (right panel). A549 cells were stained with ALDeflour reagent either in the absence or presence of DEAB (for negative control) and followed by FACS analysis (lower panel). (**b**) Percentage of SP, CD133^{pos} primary adenocarcinoma cells was determined by FACS after 1 week of sphere culture (left panel). The percentage of SP, CD133^{pos} cells was determined by FACS after culturing in adherent culture conditions for 2 weeks (middle panel) or 4 weeks (right panel). (**c**) A549 cells (left panel) or primary adenocarcinoma cells (right panel) were co-stained with Hoechst dye and CD133 antibody, and the percentage of CD133^{pos} cells in SP and non-SP cells was determined by FACS. (**d**) A549 cells (left panel) or primary adenocarcinoma (right panel) SP and non-SP cells were isolated and subsequently stained with ALDeflor reagent. The percentage of ALDH^{high} cells in SP or non-SP cells was determined by FACS. All FACS assays were performed in triplicates and error bars represent S.D. Data are representative of three independent experiments. (ns: non significant, **$P < 0.01$)

CD133pos cells were compared with 500 000 non-sorted cells (containing ∼10% SP and ∼2% CD133pos cells, respectively), we consistently observed higher colonization activities by the non-sorted cells (Supplementary Figures S1C and S1D), suggesting that enrichment of CS/PCs by one marker only represents a fraction of CS/PC activity of the bulk population.

Phenotypically distinct CS/PC subpopulations exhibit distinct self-renewal and metastatic gene expression patterns. As different marker-defined CS/PC subpopula-

tions appear to represent non-overlapping cells, we examined if different CS/PC subpopulations display distinct gene expression patterns. SP cells displayed increased *oct4* and *nanog* expression compared with non-SP cells in both A549 and primary NSCLA cells (Figure 2a left and right panels, respectively). A549 CD133pos cells had increased *oct4* and *nanog* expression compared with CD133neg cells (Figure 2b, left panel). In primary NSCLA CD133pos cells, we observed an increase in *nanog* and *hes1* expression (Figure 2b, right panel). Consistent with previous observations by Sullivan *et al.*,[13] we observed increased *notch1* expression
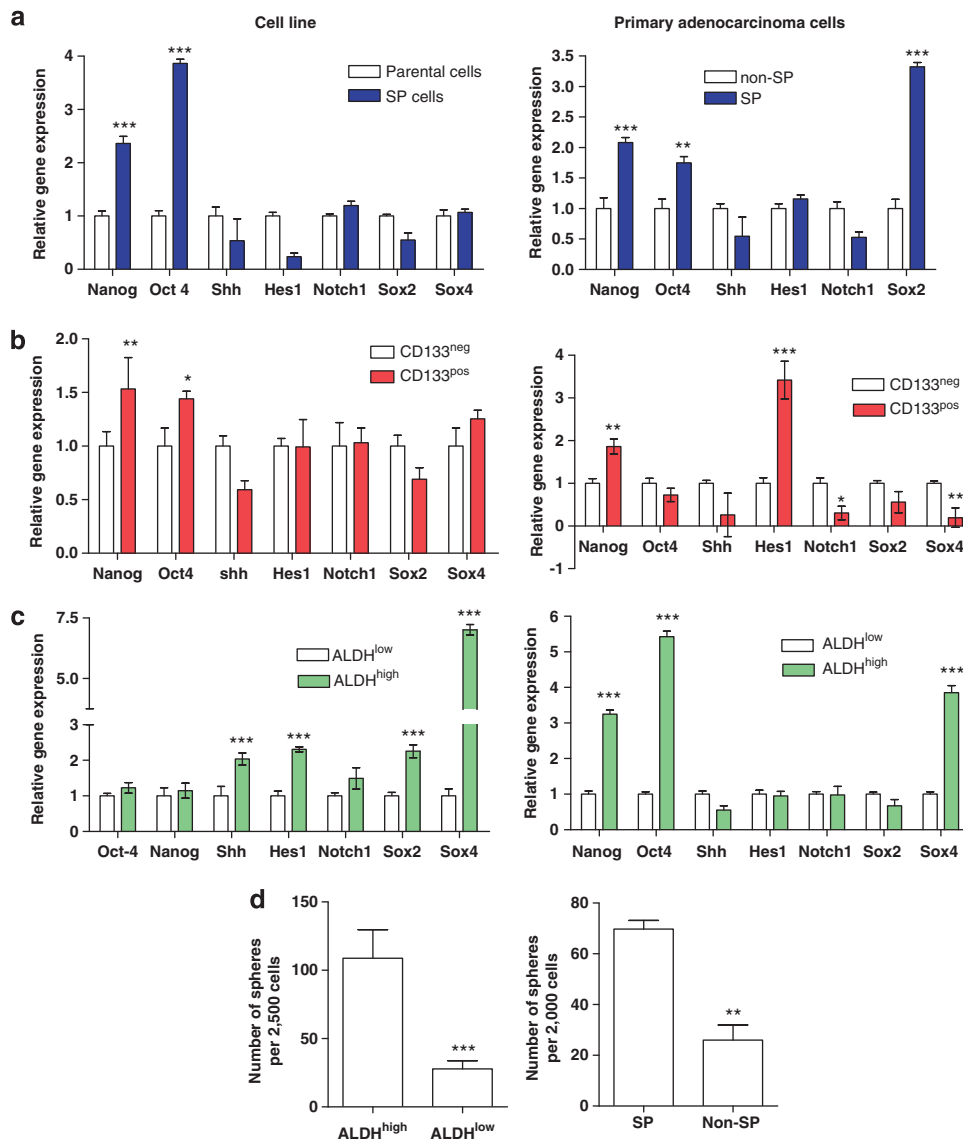
Figure 2 Different subpopulations of CSC-marker expressing cells display distinct patterns of self-renewal gene expression and sphere-forming activities. (**a**) The SP and non-SP cells from A549 (left panel) or primary adenocarcinoma cells (right panel) were sorted for RNA isolation. A panel of self-renewal gene expression was assessed by qPCR analysis. (**b**) CD133pos and CD133neg cells were sorted from A549 (left panel) or primary adenocarcinoma cells (right panel) and the expression of a panel of self-renewal genes was determined by qPCR. (**c**) ALDHhigh and ALDHlow cells were sorted from A549 (left panel) or primary adenocarcinoma cells (right panel), and the expression of self-renewal genes was determined by qPCR. The relative gene expression was determined by calculating fold change in gene expression from control sample, normalized to GAPDH expression. Above are representative of two independent experiments and error bars represent S.D. (*$P < 0.05$, **$P < 0.01$, ***$P < 0.001$). (**d**) Primary adenocarcinoma cells were sorted for SP and non-SP cells (left panel), or ALDHhigh and ALDHlow cells (right panel), and were cultured in non-adherent sphere culture conditions. The number of spheres formed after 15 days was determined by quantification under a light microscope. Above are representative of two independent experiments and error bars represent S.D. (**$P < 0.01$, ***$P < 0.001$)

in ALDH^{high} cells compared with ALDH^{low} A549 cells. Additionally, we observed increased *hes1* and *shh* expression in ALDH^{high} cells (Figure 2c, left panel). Interestingly, in primary NSCLA cells, the ALDH[high] population had increased *oct4* and *nanog* expression, but not *notch1*, *hes1* or *shh* gene expression, compared with ALDH^{low} cells. Consistent with the increased expression of self-renewal genes, SP and ALDH[high] subpopulations displayed significantly increased sphere-forming activities compared with non-SP and ALDH^{low} cells, respectively (Figure 2d, left and right panels, respectively). These results suggest that different CS/PC subpopulations exhibit distinct patterns of self-renewal genes for tumor-initiating cell propagation.

Recent studies suggest that CSCs may serve as the 'seeds' for tumor metastasis at the secondary site.[18,19] We therefore examined the expression of metastasis-associated genes in different CS/PC subpopulations. SP cells from primary NSCLA cells had increased expression of *CXCR4*, *HoxB9*, *TGFβ1*, *VEGFA* and *IL-6* compared with non-SP cells (Figure 3a), whereas CD133^{pos} cells had increased expression of IL6 alone compared with CD133^{neg} cells (Figure 3b). ALDH^{high} cells yielded a distinct metastasis-associated gene (including *TNFα*, *HoxB9*, *VEGFA* and *IL-6*) expression profile compared with ALDH^{low} cells (Figure 3c). To examine whether the expression of metastasis-associated genes are reflective of the *in vivo* metastatic capacity of these CS/PC subpopulations, we performed the lung colonization assay. Consistent with our previous observations,[10] SP cells had increased lung colonization activity compared with non-SP cells, and CD133^{pos} cells demonstrated an increased lung colonization compared with CD133^{neg} cells (Figure 3d, left panel). Regardless, no difference between ALDH^{low} and ALDH^{high} cells in a lung colonization activity was detected

(Figure 3d, right panel). However, ALDH[high] cell-injected mice developed numerous liver tumors (seven out of the eight mice injected had liver tumors), whereas mice injected with ALDH^{low} cells did not develop any liver tumors. Therefore, multiple CS/PC subpopulations may have distinct metastatic gene expression patterns and metastasis activities.

Marker-defined NSCLA CS/PC and non-CS/PC subpopulations are interconvertible. Although NSCLA SP cells display significantly higher tumorigenic activity than non-SP cells in the lung colonization assay, the non-SP cells still formed tumors in xeno-transplanted mice.[10] This phenomenon can be explained by either the existence of tumor-initiating cells in non-SP pool (e.g., defined by expression of other CS/PC markers) or by a possible conversion of non-SP to SP cells. To examine the later possibility, we isolated non-SP cells and confirmed their purity (>99.8%) by FACS analysis. When cultured in adherent culture conditions, these isolated non-SP cells generated SP cells to the extent of parental cells in 7 days (Supplementary Figure S2A). To perform a more stringent analysis, we isolated green-fluorescent protein[pos] (GFP^{pos}) SP cells and GFP[neg] non-SP cells, and when co-cultured at 1:1 ratio, GFP[neg] non-SP cells gave rise to GFP^{neg} SP cells after several cell doublings (Figure 4a). Furthermore, clones generated from single non-SP cells expressed a significant fraction of SP cells (2–30% in A549 cells, Figure 4b, left panel; 5–38% for primary NSCLA cells, Figure 4b, right panel). Importantly, non-SP cells generated SP cells *in vivo* in xenografted mice (Figure 4c). Such a dynamic conversion between marker-defined non-CS/PCs and CS/PCs was also observed in other non-CSPC/CSPC populations like
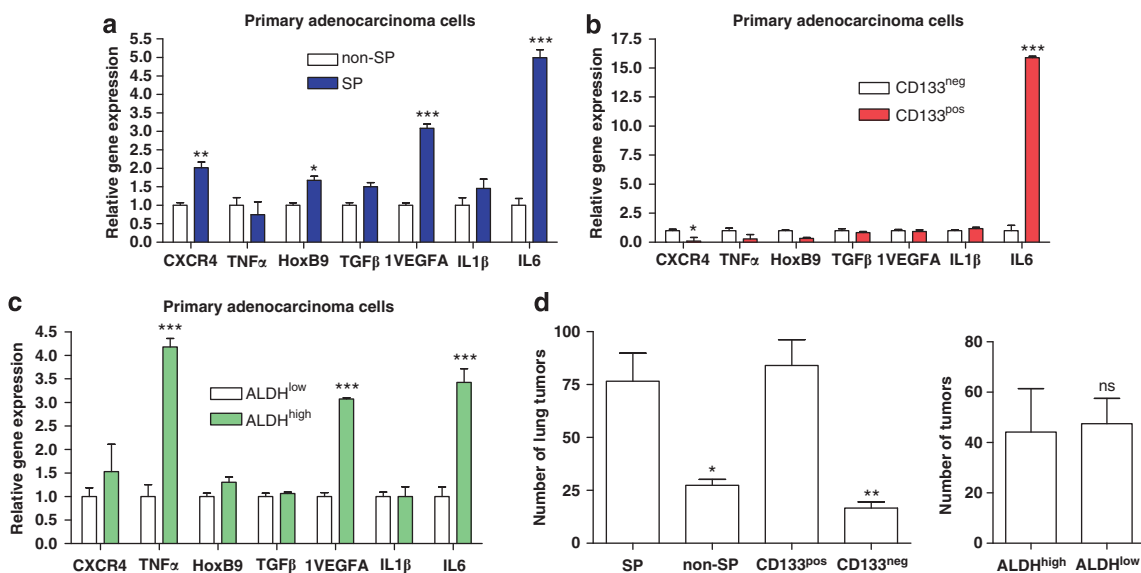
Figure 3 Different subpopulations of CSC-marker expressing cells display distinct patterns of metastatic gene expression and lung colonization activities. (**a–c**) Primary adenocarcinoma cells were either sorted for SP and non-SP cells (**a**), ALDH^{high} and ALDH^{low} cells (**b**) or CD133^{pos} and CD133^{neg} cells (**c**). The relative gene expression was determined by qPCR. All assays were performed in triplicates and error bars represent S.D. The results are representative of three independent experiments. (**d**) A total of 10 000 SP, non-SP, CD133^{pos} or CD133^{neg} cells (left panel), and 10 000 ALDH^{high} or ALDH^{low} cells (right panel) of A549 were sorted and injected intravenously into NSG mice (*n* = 6 per condition). After 12 weeks, lungs were dissected and the number of lung tumors was quantified to determine the lung colonization activity. Error bars represent S.E.M. (*P<0.05, **P<0.01, ***P<0.001)
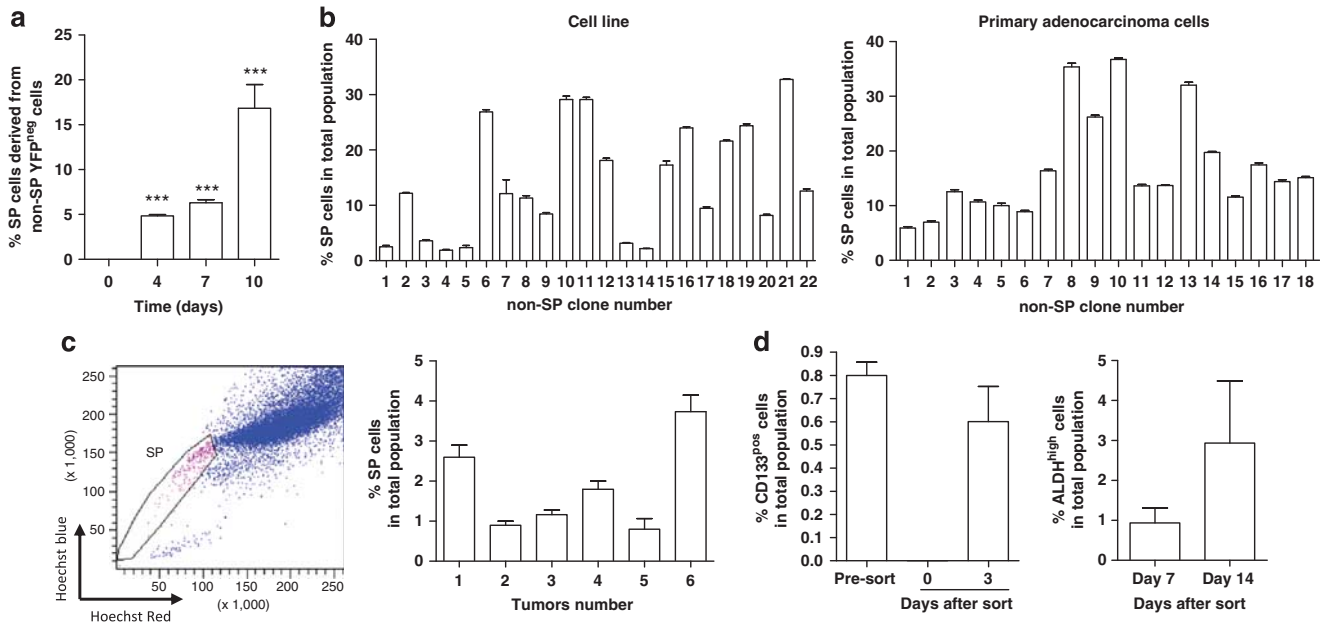
Figure 4 CSCs and non-CSCs are plastic with distinct transition kinetics among different marker-defined CSCs. (**a**) A549 cells were infected with EGFP expressing vector and after 4 days, cells were stained with Hoechst dye. Equal numbers of GFP^{pos} SP cells sorted to 100% purity were mixed with GFP[neg] non-SP cells. SP cells derived from GFP[neg] non-SP cells was determined at different time points (day 0, 4, 7, 10) by FACS analysis. Above is a representative of two independent experiments and error bars represent S.D. (*** $P < 0.001$). (**b**) A549 cells (left panel) or primary adenocarcinoma cells (right panel) were stained with Hoechst dye and non-SP cells were sorted into a 96-well plate with a single cell per well. Non-SP clones grown from single cells were analyzed by FACS to determine the percentage of SP cells. (**c**) Isolated A549 non-SP cells were injected subcutaneously into immune-compromised NSG mice and tumors were formed after 8 weeks. SP cells derived from non-SP cells *in vivo* were determined by FACS analysis. (**d**) Left panel: A549 cells were stained with CD133 antibody and the CD133^{neg} cells were isolated by FACS. The purity of the isolated cells was determined by re-staining cells with CD133 antibody and FACS analysis. Sorted cells were cultured in adherent culture conditions. On day 3, cells were stained with the CD133 antibody and analyzed by FACS. (**d**) Right panel: A549 cells were stained with ALDeflor reagent and ALDH^{low} cells were sorted by FACS. The purity of the isolated cells was determined by FACS analysis and sorted cells were cultured in an adherent culture condition. On days 7 and 14, cells were stained with ALDeflor reagent and analyzed by FACS to determine the percentage of ALDH^{high} cells. FACS analysis was performed in triplicates and error bars represent S.D. Data are representative of three independent experiments

CD133^{neg}/CD133^{pos} (Figure 4d left panel), ALDH^{low}/ALDH^{high} (Figure 4d right panel) and CD24^{high}CD44^{high}/CD24^{low}CD44^{high} cells (Supplementary Figure S2B). Interestingly, the conversion kinetics varied among the different marker-defined CS/PC subpopulations (Figure 4d, Supplementary Figure S2B). These results indicate that non-CS/PC and CS/PC populations are plastic and inter-convertible in lung cancer cell lines and primary NSCLAs.

EMT differentially regulates different marker-defined CS/PC subpopulations. In breast cancer cells, EMT promotes CSC transition.[17] To examine the role of EMT in the plasticity of NSCLA CS/PC, we treated A549, H441 and primary NSCLA cells with TGFβ1 to induce EMT. TGFβ1 induces clear morphological changes consistent with a mensenchy-mal gene transcription profile in A549 and primary NSCLA cells (Supplementary Figure S3A left and right panels, respectively), as well as H441 cells (Supplementary Figure S3D lower panel). These morphological changes were accompanied by a decrease in E-cadherin expression and an increase in expression of mesenchymal genes like *Foxc2, N-cadherin, Twist, Snail* and *fibronectin* (Supplementary Figure S3B, A549 and H441 cells; Supplementary Figure S3C, primary NSCLA cells). E-cadherin, fibronectin and vimentin expression changes were also confirmed by immunostaining (Supplementary Figure S3D). The TGFβ1-induced EMT was transient and reversible, as

the withdrawal of TGFβ1 resulted in a reversal of the gene expression profile (Supplementary Figure S3B). The dynamic nature of TGFβ1-induced EMT was previously described,[20–22] and we observed a similar time course in correlation between morphologic changes and *EMT* markers gene expression.

Next, we examined the effect of EMT on expression of various CS/PC markers. TGFβ1 treatment increased CD133^{pos} and ALDH^{high} subpopulations in A549 cells (Figures 5a and b, respectively) and this effect was reversible during mesenchymal to epithelial transition trig-gered by TGFβ1 withdrawal. Similar to the observations of Mani *et al.*[17] in HMEC cells, we found that TGFβ1 treatment increased CD24^{low}CD44^{high} cells in A549 cells (Supplementary Figure S4A), whereas TGFβ1 withdrawal decreased the population of CD24^{low}CD44^{high} cells.

We further tested the effect of EMT on the SP subpopula-tion of CSCs. Surprisingly, TGFβ1 treatment abolished SP cells in A549 (Figure 5c, top and bottom left panel), H441 (Supplementary Figure S5A, left panel) and primary NSCLA cells (Figure 5c, bottom right panel). Consistent with the decrease in dye-exclusion, we observed a decrease in *ABCG2* transporter gene expression in A549 (Figure 5d), H441 (Supplementary Figure S5A, right panel) and primary NSCLA cells (data not shown). Accompanying the reversal of EMT upon TGFβ1 withdrawal, the dye-exclusion activity (i.e., SP cells) and *ABCG2* expression were restored to level
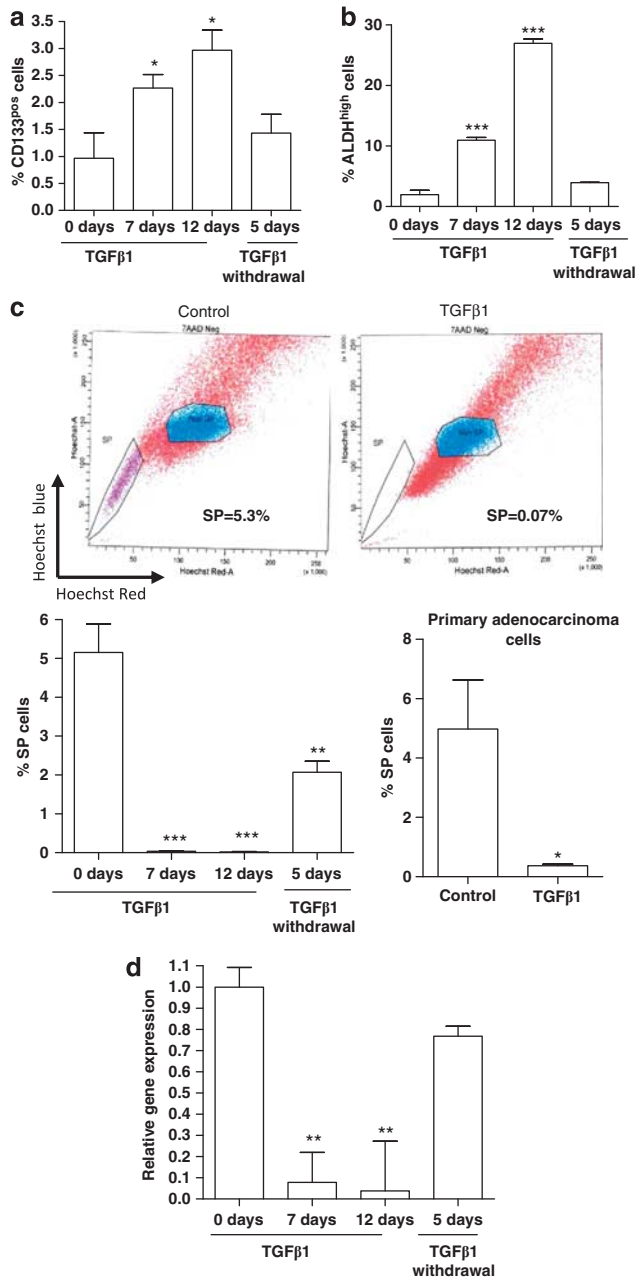
Figure 5 TGFβ1 induced EMT differentially affects different CSC subpopulations. (**a** and **b**) Cells treated with TGFβ1 for different time points were analyzed by FACS to determine CD133^pos (**a**) or ALDH^high (**b**) cells. (**c**) SP analysis was performed on control or TGFβ1 treated A549 cells by FACS (top panel). Quantification of SP analysis from TGFβ1 treated A549 cells (bottom left panel) and primary adenocarcinoma cells (bottom right panel). (**d**) RNA was isolated from TGFβ1-treated A549 cells and *ABCG2* gene expression was determined by qPCR. Above are representative of three independent experiments and error bars represent S.D. (*$P<0.05$, **$P<0.01$, ***$P<0.001$)

of control cells (Figures 5c and d). In parallel, we observed a relative decrease in cisplatin resistance after TGFβ1 treatment with a fraction of the cells remaining viable at the higher concentrations of the drug (Supplementary Figure S5B),

suggesting the presence of a drug-resistant pool in TGFβ1-treated cells. To rule out possible non-specific effects of TGFβ1 on ABC transporters, we further tested the effect of inducible Snail expression. 4-OH tamoxifen induced an EMT phenotype in Snail-ER/A549 cells (Supplementary Figure S6A), as evidenced by reduced *E-cadherin* expression and increased *FoxC2*, *fibronectin* expression. The Snail induced EMT decreased both SP cells (Supplementary Figure S6B) and *ABCG2* expression (Supplementary Figure S6C), similar to the TGFβ1 treatment. We conclude that EMT decreases SP cells in NSCLAs while increasing other CS/PC subpopulations.

As EMT differentially regulates various CS/PC subpopulations, we wanted to address if these different CS/PC subpopulations vary in their EMT marker expression. Interestingly, SP cells showed increased E-cadherin but decreased Snail and Twist expression compared with non-SP cells (Supplementary Figure S7A). CD133^pos (Supplementary Figure S7B) and ALDH^high (Supplementary Figure S7C) cells had increased Twist and Snail expressions compared with CD133^neg and ALDH^low cells, respectively. These observations suggest that SP cells are more epithelial-like, whereas CD133^pos and ALDH^high cells are more mesenchymal-like cells. The results reaffirm that SP cells represent a distinct CS/PC subpopulation from that of CD133^pos or ALDH^high CS/PCs, and support that EMT is a potential mechanism involved in regulating the plasticity of various marker-defined CS/PC subpopulations in NSCLAs.

EMT induces self-renewal, metastatic gene expression and the CS/PC activity. With differential effects of EMT on various CS/PC subpopulations, we examined the role of EMT on CS/PC activity by assessing the self-renewal gene expression pattern after TGFβ1 treatment. TGFβ1 treatment increased *oct4*, *nanog* and *notch1* expression compared with untreated cells (Figure 6a), whereas the self-renewal gene expression was reversed to control levels upon the withdrawal of TGFβ1 (Supplementary Figure S8). We observed a close correlation between the morphological changes during EMT process and self-renewal gene expression. Consistent with the EMT promoting self-renewal gene expression, we found a significant increase in sphere-forming activity in TGFβ1-treated H441 and primary NSCLA cells (Figure 6b, left and right panels, respectively). Concomitantly, TGFβ1 treatment also increased the expression of several metastatic genes including *HoxB9*, *TGFβ1*, *VEGFA*, *IL-1β* and *IL-6* (Figure 6c), and enhanced lung colonization activity (Figure 6d). These results indicate that EMT can serve as a mechanism of plasticity in defined subpopulations of CS/PCs promoting tumor initiation and metastasis. Interestingly, TGFβ1-treated cells appeared more prone to liver tumor development in mice similar to ALDH^high cells (data not shown). However, because these xenografts were generated through intra-venous injection, we cannot determine if the liver tumors were derived from lung metastasis or from liver-lodged cancer cells.

Rac1 targeting blocks EMT and inhibits CS/PC activities. Rac1 is a critical regulator of cell cytoskeletal organization and transcriptional regulation. As EMT involves distinct
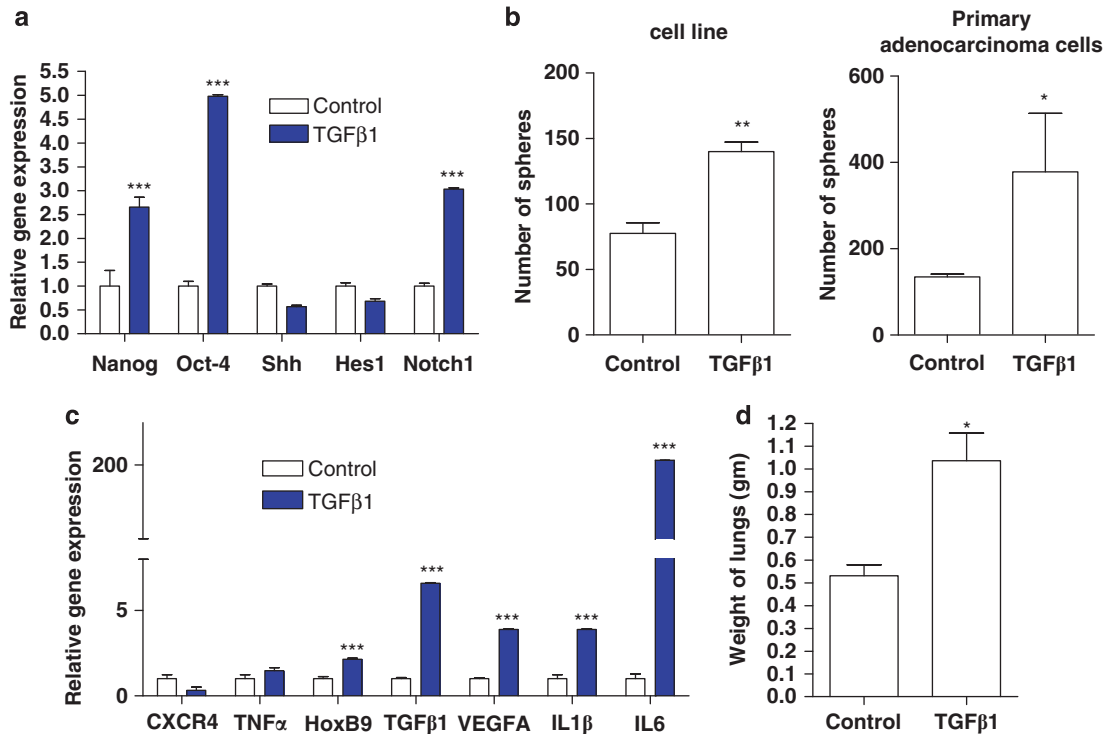
Figure 6 TGFβ1-induced EMT increases the expression self-renewal and metastatic genes and the CSC activity. (**a**) qPCR was performed on RNA isolated from A549 control and TGFβ1-treated cells for an analysis of self-renewal gene expression. (**b**) H441 (left panel) and primary human lung adenocarcinoma cells (right panel) were treated with vehicle or TGFβ1 for 12 days and were subsequently plated for sphere culture. The number of spheres formed after 15 days were counted under light microscope. (**c**) qPCR was performed on RNA isolated from primary adenocarcinoma control and TGFβ1-treated cells to determine the differences in the expression of several metastatic genes. All assays were performed in triplicates and error bars represent S.D. (*$P < 0.05$, **$P < 0.01$, ***$P < 0.001$). Data are representative of three independent experiments. (**d**) A549 control or TGFβ1-treated cells were injected intravenously into NSG mice ($n = 8$ per condition). The number of tumors formed in the lungs was determined after 10–12 weeks. Error bars represent S.E.M. (*$P < 0.05$)

morphological and transcription alterations, we wanted to determine whether Rac1 is involved in the NSCLA EMT process. We previously showed that Rac1 regulates cell adhesion, migration and lung colonization, and is required for metastasis of NSCLA cells.[10] TGFβ1 treatment increased active Rac1-GTP level in A549 cells reversibly, consistent with the transient nature of TGFβ1 on EMT (Figure 7a). Rac1 knockdown mediated by shRNA blocked the actin-cytoskeletal restructuring during EMT (data not shown). Rac1 knockdown was able to block the EMT gene signature changes such as *E-cadherin* reduction and *Snail* enhancement (Figure 7b left and right panels, respectively). Accompanying the blockade of EMT by Rac1 knockdown, we observed a significant decrease in sphere-forming activity (Supplementary Figure S9) and decrease in lung colonization by H441 (data not shown) and primary NSCLA cells. These changes initiated by Rac1 suppression improved the survival of xenograft mice (Figure 7c). NSC23766, a Rac inhibitor, decreased Rac1 activity in A549 cells (Figure 7d); consequently, partially blocked TGFβ1-induced EMT determined by marker gene expressions (Figure 7e). Further, NSC23766 inhibited the TGFβ1-induced changes in CS/PC subpopulations, that is, a decrease in SP cells (Figure 7f, left panel) and an increase in ALDH^{high} cells (Figure 7f, right panel). Therefore, Rac1 constitutes a potential target in suppressing EMT-associated CS/PC plasticity.

Discussion

This study demonstrates that drug-resistant SP cells represent a phenotypically distinct CS/PC subpopulation from several other CS/PC subpopulations including CD133^{pos}, ALDH^{high} or CD24^{low}CD44^{high} cells in NSCLA cells. The CS/PC subpopulations are plastic, and non-CS/PCs can convert to CS/PCs under defined conditions. One possible mechanism for the dynamic transition, EMT, can differentially regulate various CS/PC subpopulations and promotes a net increase of CS/PC activity *in vitro* and *in vivo*. Our work implies that the elimination of one CS/PC subpopulation may be insufficient for cancer eradication, because other CS/PC subpopulations, as well as plastic conversion of non-CS/PCs, could potentially propagate tumors. Thus, effective inhibition of CS/PC activity and the dynamic conversion of non-CS/PCs to CS/PCs may be necessary to achieve NSCLA eradication. To this end, we show that Rac1 GTPase, an EMT regulator, may be a useful target for suppressing multiple subpopulations of CS/PCs and CS/PC plasticity.

Clinical observations of secondary metastasis developing post-surgery or chemotherapy have spawned the hypothesis that these metastases are derived from a therapy-resistant tumor cells. CSC theory (reviewed in Shackleton *et al.*[1]) proposes that irrespective of cellular origin, cancer cells, like normal stem cells, are hierarchically organized. In organs like
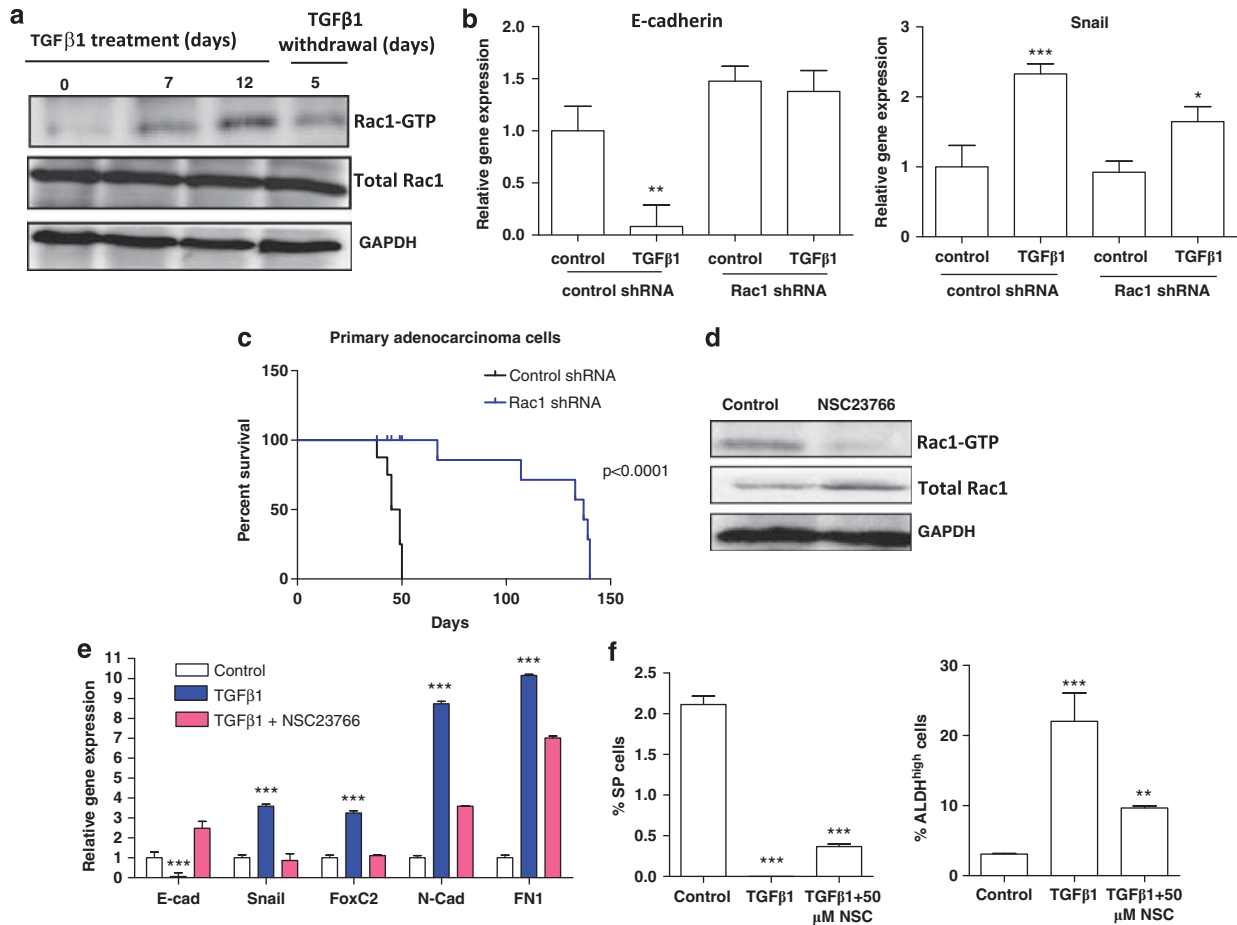
Figure 7 EMT-mediated plasticity is regulated by Rac1 GTPase. (**a**) Cell lysates were collected from control, TGFβ1 treated or TGFβ1 withdrawn A549 cells and Rac1-GTP pull-down assay was performed. Total Rac1 and GAPDH were used as loading controls. (**b**) A549 cells infected with lentivirus-expressing control or Rac1 shRNA were either treated with vehicle or TGFβ1 for 7 days and lysed for RNA isolation for qPCR analysis of E-cadherin (left panel) or snail (right panel) expression. Fold change in gene expression was determined after normalizing to GAPDH expression. (**c**) Primary adenocarcinoma patient cells infected with either control or shRNA were injected intravenously into NSG mice ($n = 8$ per group). Survival of the injected mice was processed using Kaplan–Meier analysis. (**d**) A549 cells were treated with 50 μM Rac inhibitor, NSC23766, for 12 h at 37 °C and Rac1-GTP activity assay was performed. Cells treated with vehicle alone were used as controls. Total Rac1 and GAPDH were used as loading controls. (**e** and **f**) A549 cells were either treated with vehicle alone or TGFβ1 or TGFβ1 and 50 μM Rac inhibitor, NSC23766, for 12 days. RNA was isolated to determine changes in epithelial and mesenchymal marker expression (**e**), stained for SP analysis (**f**, left panel) or stained for ALDH analysis (**f**, right panel). All assays were performed in triplicates and error bars represent S.D. (*$P < 0.05$, **$P < 0.01$, ***$P < 0.001$). Data are representative of three independent experiments

the lung, where normal stem/PC hierarchy remains unclear, it is difficult to assess whether lung adenocarcinomas fit the CSC or clonal selection model of tumor progression. In our current study, increased lung colonization and expression of metastasis-associated genes in different NSCLA CS/PC subpopulations correspond with higher metastatic potential of CS/PCs. Previous lung CSC studies[2,3,11,13] focused on single CS/PC subpopulations without examining other distinct CS/PC subpopulations that might or might not share the characterized properties. As we observed minimal overlap between various NSCLA CS/PC subpopulations, two possibilities remain. First, the CS/PC subpopulations examined might represent a plastic pool of cancer progenitors, not *bona fide* CSCs. Second, lung CSCs might express multiple CSC markers but a truly identifying marker combination remains unknown.

Drinks *et al.*[28] discussed CSC plasticity and postulated that the unstable genomic environment in cancer cells might readily facilitate reprogramming from differentiating cancer cells to CSCs, unlike the hurdle of differentiated cells reprogramming into induced pluripotent stem cells. Boiko *et al.*[27] reported CD271+ CSC marker in human melanoma, with CD271− cells displaying slower tumor growth in human skin grafts in immunodeficient mice. However, the CD271− cells derived from *in vitro* or *in vivo* cultured patient cells resulted in increased tumorigenic potential. CSC plasticity was also supported by studies of Roesch *et al.*[15] in melanoma cells, where JARID 1B^{neg} cells could readily convert to JARID 1B^{pos} cells, indicating that the cell heterogeneity in tumor growth is a dynamic process mediated by a temporary CSC pool. Similarly, Iliopoulos *et al.*[29] have demonstrated that non-CSC pools, defined by CD24^{high}CD44^{high} cells in breast cancer and CD133^{low}CD44^{low} in prostate cancer, can convert to CD24^{low}CD44^{high} and CD133^{high}CD44^{high} CSCs, respectively, in an IL6-dependent manner. Our work here presents the first study that stringently demonstrates the plasticity

between multiple NSCLA non-CS/PC and CS/PC subpopulations, and supports a model describing the stochastic transition of breast cancer cells.[30]

Recent breast cancer studies suggest that EMT can promote stem cell characteristics in mammary cancer cells.[17] Our current study demonstrates that EMT promotes CS/PC activity in NSCLAs and extends the observations of a single CSC marker to multiple CS/PC subpopulations and show that EMT differentially regulates CS/PC subpopulations, promoting some (e.g., CD133^{pos}, ALDH^{high} and CD24^{low}CD44^{high}) while suppressing others (e.g., SP). The observed decrease in SP cells and ABCG2 expression in the mesenchymal state of NSCLA cells is consistent with the reported inhibitory effect of TGFβ1 on SP cells and ABCG2 expression in breast cancer cells.[22] Interestingly, our observed self-renewal gene increase correlates with the findings that oct4 and nanog overexpression induces EMT in NSCLA cells.[31] Furthermore, our observed increase in IL6 expression by TGFβ1 treatment in CS/PCs corroborates with another report, where TGFβ1 was shown to induce EGFR inhibitor resistance in H1650 lung adenocarcinoma cells mediated by IL6.[32] However, our approach using primary NSCLA samples to confirm our cell line-based observations strengthens the pathological relevance of the conclusions in understanding the chemoresistant lung cancer cells.

We observed an increase in IL1β expression after TGFβ1 treatment. It is possible that TGFβ1 regulates expression of cytokines including IL1β through the NF-$\kappa\beta$ pathway. In keratinocytes, Snail, through its RelA domain activity, can regulate NF-$\kappa\beta$ activity and modulate cytokine expression.[23] Similarly, IL6 is increased in all CS/PC subpopulations and TGFβ1-treated cells, which could serve as a common signaling axis contributing to CS/PC metastasis. Previously, increased IL6 expression was associated with EMT induced either by TGFβ1 or Snail/Zeb1 in H358 lung adenocarninoma cells.[24] In human trabecular meshwork cells, TGFβ1 was shown to induce IL6 expression and secretion.[25] Interestingly, IL6 overexpression in breast adenocarcinoma cells resulted in a 5–7-fold increase in lung metastases in xenograft models.[26] Based on these observations, it is possible that increased IL6 expression downstream of TGFβ1 is involved in lung adenocarcinoma metastasis.

Among the potential molecular pathways regulating CS/PC plasticity, we found Rac1 GTPase, a tractable candidate critical for the EMT-mediated non-CS/PC to CS/PC transition. Rac1, together with RhoA, has an important role in EMT, during which cells undergo profound morphological changes and acquire a migratory phenotype.[33] An active isoform of Rac1, Rac1b, has been shown to mediate EMT and ROS production,[34] and more recently Rac1 was shown to regulate TGFβ1-mediated EMT and MMP9 production in transformed keratinocytes.[35] Our finding that Rac1 inhibition can block EMT-mediated changes in CS/PCs raises an intriguing idea that targeting Rac1 signaling might present a novel therapeutic strategy for reducing CS/PC plasticity, in addition to suppressing CS/PC activity by inhibiting the cell cycle progression of CS/PC self-renewal process.[10] The impact of such a concept on cancer therapeutics will await further validation in in vivo conditions where dynamic changes may constantly favor CS/PC selection and progression.

Materials and Methods

Cell culture. A549 and H441 cells were cultured according to ATCC guidelines. Primary patient lung adenocarcinoma samples were obtained with written consent from patients under an approved Institution Review Board protocol by the University of Cincinnati Scientific Review Committee (IRB no. 01–09–27–07), and were used in the experiments according to the Cincinnati Children's Hospital Medical Center Scientific Review Committee (IRB no. 07–06–57) that the identity of the patients remains anonymous. Detailed methods are described in Supplementary Materials section.

SP, ALDH and CD133 cell analysis and isolation. Cells were either stained with Hoechst 33342 staining buffer for SP as described previously[36] at a final concentration of 5 μg/ml Hoechst 33342, or Aldeflor reagent (Stem Cell Technologies, Inc., Vancouver, BC Canada) according to manufacturer's guidelines for ALDH^{high} cells or anti-CD133/1 antibody (Miltenyi Biotec Inc., Auburn, CA, USA) for CD133^{pos} cells. The cells were either analyzed or sorted for SP/ALDH^{high}/CD133^{pos} cells by FACS with either FACS Canto bench top or FACS Ariel sorter (BD, Franklin Lakes, NJ, USA).

Rac1-GTP pull-down assay. To perform Rac1 pull-down assays, cells were lysed by adding lysis buffer (20 mM Tris HCl pH 7.6, 100 mM NaCl, 10 mM MgCl, 1% Triton X-100, 0.2% SDS) with protease and phosphatase inhibitors directly to adherent cells as described previously.[37] The lysates are incubated with bead-immobilized P21-binding domain of a downstream effector protein, PAK1. After washes, Rac1-GTP bound to the beads and total lysates are loaded into parallel gels to reveal relative Rac1-GTP and Rac1 contents by anti-Rac1 western blotting. GAPDH was probed in the total lysates to ensure equal loading.

Lung colonization assay. Use of mice as xenograft hosts was approved by the IACUC committee at the Cincinnati Children's Hospital Medical Center (Protocol no. 8D06052). Specified number of cells were suspended in PBS and injected intravenously into immune compromised NOD/SCID/γc$^{-/-}$ (NSG) mice by tail vein injection. At the end of the study, lungs were fixed in Bouin's solution to count the number of tumors.

Statistics. Statistical analysis was performed either by Student's t-test or two-way ANOVA Bonferroni test.

Conflict of Interest
The authors declare no conflict of interest.

1. Shackleton M, Quintana E, Fearon ER, Morrison SJ. Heterogeneity in cancer: cancer stem cells versus clonal evolution. Cell 2009; **138**: 822–829.
2. Eramo A, Lotti F, Sette G, Pilozzi E, Biffoni M, Di Virgilio A et al. Identification and expansion of the tumorigenic lung cancer stem cell population. Cell Death Differ 2008; **15**: 504–514.
3. Ho MM, Ng AV, Lam S, Hung JY. Side population in human lung cancer cell lines and tumors is enriched with stem-like cancer cells. Cancer Res 2007; **67**: 4827–4833.
4. Sun Y, Zheng S, Torossian A, Speirs CK, Schleicher S, Giacalone NJ et al. Role of insulin-like growth factor-1 signaling pathway in Cisplatin-resistant lung cancer cells. Int J Radiat Oncol Biol Phys 2012; **82**: e563–e572.
5. Lapidot T, Sirard C, Vormoor J, Murdoch B, Hoang T, Caceres-Cortes J et al. A cell initiating human acute myeloid leukaemia after transplantation into SCID mice. Nature 1994; **367**: 645–648.
6. Singh SK, Hawkins C, Clarke ID, Squire JA, Bayani J, Hide T et al. Identification of human brain tumour initiating cells. Nature 2004; **432**: 396–401.
7. Al-Hajj M, Wicha MS, Benito-Hernandez A, Morrison SJ, Clarke MF. Prospective identification of tumorigenic breast cancer cells. Proc Natl Acad Sci USA 2003; **100**: 3983–3988.
8. O'Brien CA, Pollett A, Gallinger S, Dick JE. A human colon cancer cell capable of initiating tumour growth in immunodeficient mice. Nature 2007; **445**: 106–110.
9. Chiba T, Kita K, Zheng YW, Yokosuka O, Saisho H, Iwama A et al. Side population purified from hepatocellular carcinoma cells harbors cancer stem cell-like properties. Hepatology 2006; **44**: 240–251.

10. Akunuru S, Palumbo J, Zhai QJ, Zheng Y. Rac1 targeting suppresses human non-small cell lung adenocarcinoma cancer stem cell activity. *PLoS One* 2011; **6**: e16951.

11. Levina V, Marrangoni AM, DeMarco R, Gorelik E, Lokshin AE. Drug-selected human lung cancer stem cells: cytokine network, tumorigenic and metastatic properties. *PLoS One* 2008; **3**: e3077.

12. Deng S, Yang X, Lassus H, Liang S, Kaur S, Ye Q et al. Distinct expression levels and patterns of stem cell marker, aldehyde dehydrogenase isoform 1 (ALDH1), in human epithelial cancers. *PLoS One* 2010; **5**: e10277.

13. Sullivan JP, Spinola M, Dodge M, Raso MG, Behrens C, Gao B et al. Aldehyde dehydrogenase activity selects for lung adenocarcinoma stem cells dependent on notch signaling. *Cancer Res* 2010; **70**: 9937–9948.

14. Gupta PB, Onder TT, Jiang G, Tao K, Kuperwasser C, Weinberg RA et al. Identification of selective inhibitors of cancer stem cells by high-throughput screening. *Cell* 2009; **138**: 645–659.

15. Roesch A, Fukunaga-Kalabis M, Schmidt EC, Zabierowski SE, Brafford PA, Vultur A et al. A temporarily distinct subpopulation of slow-cycling melanoma cells is required for continuous tumor growth. *Cell* 2010; **141**: 583–594.

16. Gupta PB, Chaffer CL, Weinberg RA. Cancer stem cells: mirage or reality? *Nat Med* 2009; **15**: 1010–1012.

17. Mani SA, Guo W, Liao MJ, Eaton EN, Ayyanan A, Zhou AY et al. The epithelial-mesenchymal transition generates cells with properties of stem cells. *Cell* 2008; **133**: 704–715.

18. Liu H, Patel MR, Prescher JA, Patsialou A, Qian D, Lin J et al. Cancer stem cells from human breast tumors are involved in spontaneous metastases in orthotopic mouse models. *Proc Natl Acad Sci USA* 2010; **107**: 18115–18120.

19. Wicha MS, Liu S, Dontu G. Cancer stem cells: an old idea–a paradigm shift. *Cancer Res* 2006; **66**: 1883–1890; discussion 1895–1886.

20. Kim JH, Jang YS, Eom KS, Hwang YI, Kang HR, Jang SH et al. Transforming growth factor beta1 induces epithelial-to-mesenchymal transition of A549 cells. *J Korean Med Sci* 2007; **22**: 898–904.

21. Rho JK, Choi YJ, Lee JK, Ryoo BY, Na II, Yang SH et al. Epithelial to mesenchymal transition derived from repeated exposure to gefitinib determines the sensitivity to EGFR inhibitors in A549, a non-small cell lung cancer cell line. *Lung Cancer* 2009; **63**: 219–226.

22. Yin L, Castagnino P, Assoian RK. ABCG2 expression and side population abundance regulated by a transforming growth factor beta-directed epithelial-mesenchymal transition. *Cancer Res* 2008; **68**: 800–807.

23. Lyons JG, Patel V, Roue NC, Fok SY, Soon LL, Halliday GM et al. Snail up-regulates proinflammatory mediators and inhibits differentiation in oral keratinocytes. *Cancer Res* 2008; **68**: 4525–4530.

24. Thomson S, Petti F, Sujka-Kwok I, Mercado P, Bean J, Monaghan M et al. A systems view of epithelial-mesenchymal transition signaling states. *Clin Exp Metastasis* 2011; **28**: 137–155.

25. Liton PB, Li G, Luna C, Gonzalez P, Epstein DL. Cross-talk between TGF-beta1 and IL-6 in human trabecular meshwork cells. *Mol Vision* 2009; **15**: 326–334.

26. Di Carlo E, Modesti A, Castrilli G, Landuzzi L, Allione A, de Giovanni C et al. Interleukin 6 gene-transfected mouse mammary adenocarcinoma: tumour cell growth and metastatic potential. *J Pathol* 1997; **182**: 76–85.

27. Boiko AD, Razorenova OV, van de Rijn M, Swetter SM, Johnson DL, Ly DP et al. Human melanoma-initiating cells express neural crest nerve growth factor receptor CD271. *Nature* 2010; **466**: 133–137.

28. Dirks P. Cancer stem cells: invitation to a second round. *Nature* 2010; **466**: 40–41.

29. Iliopoulos D, Hirsch HA, Wang G, Struhl K. Inducible formation of breast cancer stem cells and their dynamic equilibrium with non-stem cancer cells via IL6 secretion. *Proc Natl Acad Sci USA* 2011; **108**: 1397–1402.

30. Gupta PB, Fillmore CM, Jiang G, Shapira SD, Tao K, Kuperwasser C et al. Stochastic state transitions give rise to phenotypic equilibrium in populations of cancer cells. *Cell* 2011; **146**: 633–644.

31. Chiou SH, Wang ML, Chou YT, Chen CJ, Hong CF, Hsieh WJ et al. Coexpression of Oct4 and Nanog enhances malignancy in lung adenocarcinoma by inducing cancer stem cell-like properties and epithelial-mesenchymal transdifferentiation. *Cancer Res* 2010; **70**: 10433–10444.

32. Yao Z, Fenoglio S, Gao DC, Camiolo M, Stiles B, Lindsted T et al. TGF-beta IL-6 axis mediates selective and adaptive mechanisms of resistance to molecular targeted therapy in lung cancer. *Proc Natl Acad Sci USA* 2010; **107**: 15535–15540.

33. Kardassis D, Murphy C, Fotsis T, Moustakas A, Stournaras C. Control of transforming growth factor beta signal transduction by small GTPases. *FEBS J* 2009; **276**: 2947–2965.

34. Radisky DC, Levy DD, Littlepage LE, Liu H, Nelson CM, Fata JE et al. Rac1b and reactive oxygen species mediate MMP-3-induced EMT and genomic instability. *Nature* 2005; **436**: 123–127.

35. Santibanez JF, Kocic J, Fabra A, Cano A, Quintanilla M. Rac1 modulates TGF-beta1-mediated epithelial cell plasticity and MMP9 production in transformed keratinocytes. *FEBS Lett* 2010; **584**: 2305–2310.

36. Goodell MA, Brose K, Paradis G, Conner AS, Mulligan RC. Isolation and functional properties of murine hematopoietic stem cells that are replicating *in vivo*. *J Exp Med* 1996; **183**: 1797–1806.

37. Guo F, Gao Y, Wang L, Zheng Y. p19Arf-p53 tumor suppressor pathway regulates cell motility by suppression of phosphoinositide 3-kinase and Rac1 GTPase activities. *J Biol Chem* 2003; **278**: 14414–14419.

Supplementary Information accompanies the paper on Cell Death and Disease website (http://www.nature.com/cddis)